Ecological Indicators 189 (2026) 115126

Contents lists available at ScienceDirect

Ecological Indicators

journal homepage: www.elsevier.com/locate/ecolind

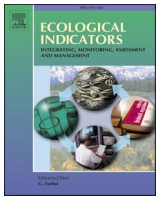

Fish trait-based indicators of mercury bioaccumulation under natural ocean acidification: Insights from a mediterranean CO_2 vent system☆

Alice Mirasole [a,1], Geraldina Signa [b,c,1], Giovanna Cilluffo [b,c,*], Cecilia Tramati [b,c], Agostino Tomasello [b,c], Antonio Mazzola [b,c], Salvatrice Vizzini [b,c]

[a] Stazione Zoologica Anton Dohrn, Department of Integrative Marine Ecology, Ischia Marine Centre, 80077, Ischia, Naples, Italy
[b] Department of Earth and Marine Sciences, University of Palermo, via Archirafi 18, 90123 Palermo, Italy
[c] CoNISMa, Piazzale Flaminio 9, 00196 Rome, Italy

ARTICLE INFO

Keywords:
Climate change
Functional traits
Heavy metal
Ichthyofauna
Pollution
Trophic position

ABSTRACT

Ocean acidification is not an isolated climate-related threat to marine organisms, as it may act in combination with other stressors such as trace element contamination. Here, we took advantage of naturally acidified conditions and mercury spill-out from the shallow CO_2 vent of Vulcano Island (Italy) to test whether fish functional traits explain contaminant dynamics better than species identity under ocean acidification scenarios. Specifically, we investigated if trophic group and mobility influence total mercury (THg) bioaccumulation and trophic transfer in fish inhabiting *Cymodocea nodosa* seagrass meadows under low and ambient pH conditions. Low-mobility benthic fish, mainly represented by invertebrate feeders and small piscivores, exhibited higher THg concentration at the vent site than at reference sites, while highly mobile zooplanktivorous fish showed no significant differences, highlighting the importance of fish mobility and local trophic benthic pathways in shaping contaminant exposure and bioaccumulation. Moreover, the relationship between trophic position and THg concentration in fish was stronger in the low pH site, indicating enhanced trophic transfer and biomagnification when Hg availability is higher. In contrast, weak or absent biomagnification in the reference sites suggests that Hg transfer depends more on contaminant availability and food web structure than trophic position alone. Overall, these findings indicate that functional traits better predict Hg bioaccumulation patterns than species identity, supporting trait-based approach to assess contaminant dynamics in future ocean acidification scenarios.

1. Introduction

Ocean acidification (OA), the climate change-driven threat resulting from the ongoing increase in atmospheric pCO_2 absorbed by the ocean, the subsequent change in seawater carbonate chemistry, and the decrease in ocean pH, can strongly affect marine biodiversity and ecosystem functioning (Gaylord et al., 2015; Peña et al., 2021; *IPCC*, 2023), with potential consequences for human health and well-being (Falkenberg et al., 2020). Furthermore, OA is not an isolated threat, as it often acts in combination with other stressors (*e.g.,* ocean warming, hypoxia, pollution; Kroeker et al., 2013). In particular, the combined effect of decreasing ocean pH and increasing pollution has been studied in several marine organisms and ecosystems (*e.g.*, Lacoue-Labarthe et al., 2009, 2011; Roberts et al., 2013; Basallote et al., 2014; Lewis et al., 2016; Shi et al., 2016). As regards trace elements, one of the main issues is the increase in their solubility and bioavailability due to altered speciation and ligand building (Nikinmaa, 2013; Zeng et al., 2015), driven by the lowering of pH and redox potential of seawater (Byrne, 2002; Lall, 2002). For instance, low pH can enhance metal desorption from organic ligands, leading to an increased influx of dissolved elements (*e.g.*, Al, Cd, Cr, Cu, Ni, Pb, Zn) into sediments and the water column (Ardelan et al., 2012). At the same time, the effects of low pH on trace element accumulation and toxicity to marine organisms can be contrasting depending on the species and life stage (Ivanina and Sokolova, 2015). For instance, low pH has been found to enhance the uptake of Ag, Zn and Hg in squid and cuttlefish embryos (Lacoue-

☆ This article is part of a Special issue entitled: 'Biodiversity & climate change' published in Ecological Indicators.

* Corresponding author.
E-mail address: giovanna.cilluffo@unipa.it (G. Cilluffo).

[1] These two authors contributed equally to this manuscript.

https://doi.org/10.1016/j.ecolind.2026.115126
Received 17 February 2026; Received in revised form 16 June 2026; Accepted 25 June 2026

Labarthe et al., 2009, 2011), while dampening Hg accumulation in some fish species (Sampaio et al., 2017). Consequently, low pH may also affect marine food webs by altering the trophic transfer of trace elements, with direct implications for trace element accumulation and biomagnification along trophic chains (Ivanina and Sokolova, 2015).

Among trace elements, mercury (Hg) is one of the most widespread and hazardous contaminants in coastal marine systems (Doney et al., 2009). Mercury can be of natural or anthropogenic origin and is highly toxic even at low concentrations. The inorganic form of Hg can accumulate in sediments where it can be biologically methylated by microorganisms to methylmercury (MeHg), which is the most toxic form of mercury because it can pass through biological membranes (Cossa et al., 2022). Although fish can accumulate passively MeHg from seawater through the gills, trophic transfer has been recognised as the main route of exposure (Zhang et al., 2012). Consequently, Hg accumulation in fish can be affected by functional traits, particularly feeding habits, which regulate trophic-specific exposure and drive biomagnification toward higher trophic positions (Lall, 2002; Power et al., 2002; Campbell et al., 2005; Nfon et al., 2009; Signa et al., 2017, 2019). Fish mobility can further modulate Hg accumulation, as pelagic and demersal species may belong to different trophic pathways, and forage over different spatial and temporal scales (Signa et al., 2017; Zurlini et al., 2025), resulting in contrasting bioaccumulation patterns. For these reasons, despite many studies have investigated the patterns of Hg bioaccumulation in fish (*e.g.*, Amundsen et al., 2023; Nalley et al., 2023), understanding Hg accumulation and transfer within food webs under future OA scenarios is particularly important given also the associated potential risk for human health (Castro-González and Méndez-Armenta, 2008; Brambilla et al., 2013). Additionally, although it is well established that fish species can serve as effective ecological indicators of the combined effects of OA and trace element contamination, the extent to which their trait-based characteristics account for relative differences in trace metal accumulation and transfer through food webs under low pH conditions remains insufficiently explored.

Volcanic CO_2 vents are naturally acidified areas, which in many cases are also characterised by the spillage of major, minor and trace elements (Boatta et al., 2013; Aiuppa et al., 2021; Falcone et al., 2022; Pichler, 2024). For this reason, they provide an opportunity to study *in situ* the effects of multiple stressors (*i.e.*, OA and trace element contamination) on species and communities (Vizzini et al., 2013; Mirasole et al., 2020; Mishra et al., 2020; Andolina et al., 2025) providing new insights into ocean functioning under future scenarios. In particular, Roberts and Pichler (2022) recently demonstrated the importance of fluid and gaseous Hg emissions at the Vulcano vent (Aeolian Archipelago, Italy), recording mean total Hg (THg) concentrations in volcanic fluids ranging from 40 to 5110 pM in the hydrothermally active area, and from 0.8 to 2.4 pM in the rest of the bay. Furthermore, under the peculiar conditions of CO_2 vents, the combined effect of acidified and reducing conditions has previously been shown to favour the accumulation of trace elements in sediments and biota (Vizzini et al., 2013; Mishra et al., 2020), with possible bioaccumulation in marine food webs (Pichler, 2024). While the environmental complexity of deep CO_2 vents has been shown to favour trace element accumulation in several marine taxa (Kádár et al., 2005, 2007; Martins et al., 2006; Tovar-Sanchez et al., 2009), much less is known about trace element accumulation and trophic transfer in shallow CO_2 vents (but see Vizzini et al., 2013; Mirasole et al., 2020; Mishra et al., 2020). Among these studies, Vizzini et al. (2013) found a clear spatial gradient of trace element contamination in sediments, with potentially harmful levels near the shallow CO_2 vent of Vulcano Island and decreasing contamination levels a few hundred metres from the vent. This gradient was reflected in primary producers at the base of the food web leaving open questions about potential adverse effects on higher-order and mobile consumers such as fish (Vizzini et al., 2013).

In this context, we followed up on research at the CO_2 vent of Levante Bay, at the Vulcano Island, belonging to the Aeolian Archipelago, one of the most active volcanic areas in the Mediterranean Sea. The shallow CO_2 vent in Levante Bay (Island of Vulcano) has been extensively studied from a geochemical and biological points of view (for a review see Aiuppa et al., 2021) and has been used as a natural laboratory to investigate the effects of ocean acidification (OA) on marine species and communities (*e.g.*, Apostolaki et al., 2014; Milazzo et al., 2016; Vizzini et al., 2017). Based on existing evidence, fish inhabiting vent areas are expected to be exposed to higher Hg levels than fish from non-vent areas due to volcanic-derived Hg inputs, and its increased Hg availability under low pH and reducing conditions (negative redox potential). Accordingly, we hypothesised that Hg accumulation and trophic transfer increase with trophic position in fish assemblages from vent areas. Additionally, we hypothesised that fish functional traits such as trophic group and mobility better explain Hg accumulation and trophic transfer patterns under OA than species identity.

To test these hypotheses, we compared one CO_2 vent site (low pH conditions) with two reference sites (ambient pH) to assess: (1) differences in Hg concentration in basal organic matter sources and low order consumers; (2) differences in Hg bioaccumulation in fish, analysed at the species level and grouped by functional traits (trophic groups and mobility); and (3) differences in the relationship between fish trophic position and Hg bioaccumulation, evaluated at both the species level and across functional trait groups.

2. Materials and methods

2.1. Study area and sampling activities

The gas composition at the primary vent in Levante Bay of Vulcano Island is dominated by CO_2 (97–99% vol.), which causes changes in the carbonate chemistry of seawater (Boatta et al., 2013), resulting in a pronounced pH gradient along the northern coast of the bay. Indeed, Apostolaki et al. (2014) found 2016 ± 72 μatm (mean ± SE), 2419 ± 6 μmol kg^{-1}, and 2495 ± 6 μmol kg^{-1} for seawater pCO_2, dissolved inorganic carbon (DIC) concentration and total alkalinity, respectively, near the vent. In contrast, the same variables showed values of 699 ± 99 μatm, 2258 ± 8 μmol kg^{-1} and 2470 ± 8 μmol kg^{-1}, respectively, at ambient pH conditions (Apostolaki et al., 2014). While the concentration of some major and minor elements (such as Ca, Mg, Sr and Zn) dissolved in seawater was comparable between sites at different pH values (Boatta et al., 2013; Mirasole et al., 2017), other minor and trace elements (such as Cr, Fe, Hg, Mn and Pb) showed greater spatial variability with maximum values close to the vent (Apostolaki et al., 2014; Falcone et al., 2022; Roberts and Pichler, 2022). Furthermore, some trace elements emitted from the vents (*i.e.*, As, Cd, Hg, Pb and Zn) tended to accumulate in the sediment and biota around the vent, facilitated by altered geochemical fluxes at the sediment-seawater interface determined by acidic and reducing conditions (Vizzini et al., 2013).

Based on the geochemical characterisation described above, sampling was carried out between September and December 2014. Three sampling sites were located at increasing distances from the CO_2 vent in Levante Bay (Fig. 1) approximately 250 m from the primary CO_2 vent (hereafter referred to as "Low pH", with a mean pH 7.80 ± 0.09), approximately 500 m from the vent ("Ctrl 1", mean pH 8.19 ± 0.03) and on the nearby island of Lipari approximately 6.5 km from the primary vent ("Ctrl 2", mean pH 8.22 ± 0.02). The two reference sites (Ctrl 1, Ctrl 2) were chosen as similar to the vent site in terms of orientation (south-east), depth (2–5 m) and habitat (*Cymodocea nodosa* meadow interspersed with small rocky boulders with macroalgae). These sites have been studied in previous research (Mirasole et al., 2017, 2020, 2021a), providing detailed information on spatial and temporal variability in environmental conditions and element distribution, which guided the experimental design in line with the recommendation of Zurlini et al. (2025). At each site, fish were collected at 2–3 m depth using small trammel nets, fish traps, and hand fishing lines deployed

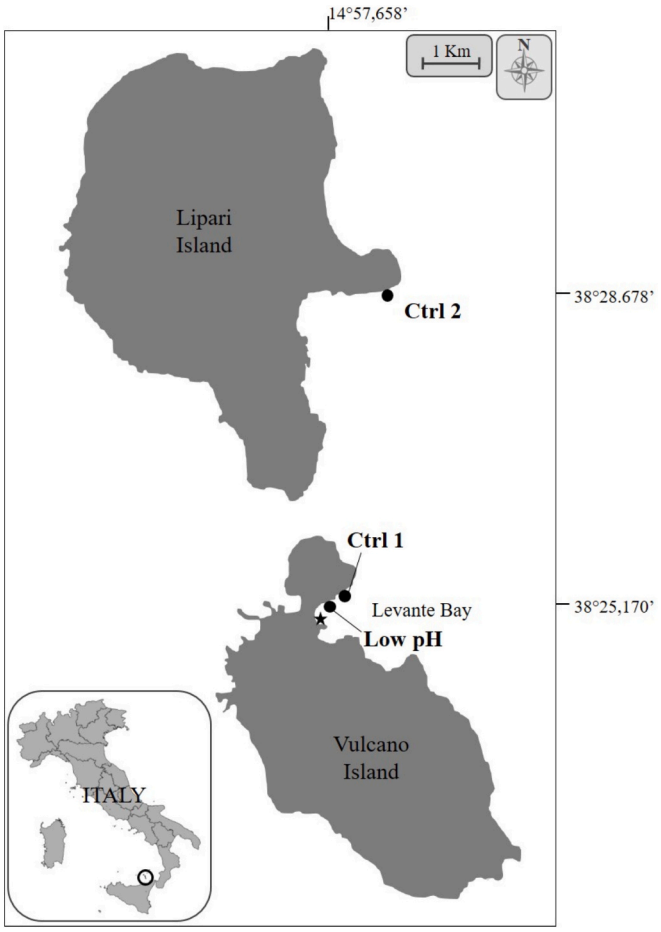

Fig. 1. - Map of the study area showing the sampling sites in Vulcano (Low pH and Ctrl 1) and Lipari Islands (Ctrl 2) (Aeolian Archipelago, Italy). The primary vent is located in Levante Bay (Vulcano) and is indicated by the star (from Mirasole et al., 2020).

once a month in September, October and December 2014 for 18–24 h (nets and traps) and 1–2 h (fishing lines). As regards low order consumers, we collected zooplankton using a plankton net (mesh size: 200 μm) towed from a small boat for 30 min at each sampling area. Surface sediment was sampled at each site using PVC hand corers (Ø 5 cm, 10 cm length, six replicates per site). The most abundant macroalgae (*Caulerpa prolifera*, *Cystoseira spp.*, *Flabellia petiolata* and *Halopteris scoparia*) and the seagrass species *Cymodocea nodosa* were collected by hand by scuba divers (three replicates per site per species). All samples were transported to the laboratory on ice and then frozen at −20 °C until analysis.

2.2. Laboratory analysis

In the laboratory, zooplankton samples were sorted under a stereomicroscope (10–40 x magnification) for whole-body analysis of the nitrogen stable isotope ratio ($\delta^{15}N$) and total mercury content (THg). Macroalgae (*Caulerpa prolifera*, *Cystoseira spp.*, *Flabellia petiolata* and *Halopteris scoparia*) and the seagrass *Cymodocea nodosa* were cleaned from epiphytes by surface scraping prior to $\delta^{15}N$ and THg analyses. Sediment samples were wet sieved at 63 μm and the fine fraction was used for THg analysis.

The fish sampled, belonging to seven families and fifteen species, were measured for total length to the nearest cm. From this pool, 3 to 6 individuals per species and site were selected based on similar size for dorsal muscle dissection and subsequent isotopic and THg analyses (Table 1). Fish species were also classified into trophic groups according to Guidetti and Sala (2007), and mobility expressed as habitat use categories (Table 1) according to Harmelin (1987). The former authors classified fish in the following trophic groups: herbivores, planktivores, detritivores, invertivores, small and large piscivores (Guidetti and Sala, 2007). On the other side, Harmelin (1987) schematised the spatial organisation of the Mediterranean ichthyofauna by defining six habitat use categories which vary along a mobility gradient from highly mobile pelagic fishes to sedentary benthic fishes namely: 1) highly mobile species living in large shoals in the water column; 2) shoaling species occupying the water column but with low horizontal mobility; 3) mesophagous demersal species with important horizontal and moderate vertical displacements (mainly Sparids); 4) nekto-benthic species living close to the bottom with very large horizontal displacements; 5) relatively sedentary mesophagous species (mainly Labrids); and 6) small, site-attached very sedentary species.

All samples (sediment, macroalgae, seagrass, zooplankton and fish muscle) were freeze-dried (ALPHA 1–4 LD plus, Martin-Christ) and ground to a fine powder using a ball mill (MM 200 Retsch). For the quantification of THg concentrations, samples were first mineralised in a microwave system (MARS 5, CEM). Sediments were mineralised using HNO_3 67–70%, H_2O_2 30%, HF 30% and Milli-Q deionised water (Method 3052, United States Environmental Protection Agency 1996), while biological tissues were mineralised using HNO_3 67–70%, H_2O_2 30% and Milli-Q deionised water. An Inductively Coupled Plasma-Optical Emission Spectrometer (ICP-OES, Optima 8000, PerkinElmer) coupled to a hydride generation system with a reducing agent, consisting of 0.2% sodium (Na) borohydride and 0.05% Na hydroxide, was used to determine THg absolute concentrations. The analytical procedure was validated against the following certified reference materials CRMs (recovery: 87–98%): sediment NIST 2702 (National Institute of Standards and Technology) for sediment samples, *Lagarosiphon major* BCR-060 (Institute for Reference Materials and Measurements) for primary producers, and fish protein DORM-4 (National Research Council of Canada) for zooplankton and fish muscle. THg concentrations were expressed as mg kg^{-1} dry weight (dw). In order to compare THg levels in commercial fish species with the European Union Maximum Residue Limits (MRLs) (Regulation EC, N. 2023/915), the THg concentration as mg kg^{-1} dw was converted to mg kg^{-1} wet weight (ww) according to Magalhães et al. (2007).

Stable nitrogen isotope ratios of zooplankton and fish samples were analysed using an Isotope Ratio Mass Spectrometer (IRMS Thermo Scientific Delta Plus XP) connected to an Elemental Analyser (Thermo Scientific Flash EA 1112). Nitrogen isotope ratios were expressed in conventional δ-unit notation ($\delta^{15}N$) as the deviation per mil (‰) from the international standard atmospheric nitrogen (N_2), according to the formula:

$$\delta^{15}N = [(^{15}N/^{14}N_{sample}/^{15}N/^{14}N_{standard}) - 1] \times 10^3.$$

The analytical precision, based on the standard deviation of the replicates of the internal standards, was 0.2‰.

2.3. Data elaboration and statistics

Considering that THg was analysed as an absolute concentration rather than as part of a compositional dataset, compositional data approaches were not applied. Differences in THg concentrations among sites (Low pH, Ctrl 1 and Ctrl 2) were first assessed using non-parametric Kruskal-Wallis test, to avoid relying on distributional assumptions, for sediment, macroalgae, seagrass, zooplankton and fish. Specifically, for fish, tests were applied on THg concentration of i) all species across sites, ii) trophic groups and iii) mobility expressed as habitat use categories. Pairwise comparisons were performed using the Mann–Whitney test. For mobility, THg concentrations were normalised to trophic position (TP) to account for within-category variability in fish trophic position (Signa et al., 2017). Habitat use categories 1 and 2 were excluded from this analysis because only one species was present in both categories.

Fish trophic position was calculated using zooplankton as a baseline by applying the following equation:

Table 1
- Summary of the fish families, species, trophic groups (Guidetti and Sala, 2007), mobility expressed as habitat use categories (*sensu* Harmelin, 1987), Maximum total length (max TL, cm) in the adult stage was also indicated for each species (Froese and Pauly, 2023), number of replicates (N), range of total length (TL, cm) and trophic position (TP) sampled in the three sites (Low pH, Ctrl 1 and Ctrl 2.

						Low pH			Ctrl 1			Ctrl 2		
Family	**Species**	**Label**	**Trophic group**	**Mobility categories***	**Max TL (cm)**	**N**	**TL (cm)**	**TP**	**N**	**TL (cm)**	**TP**	**N**	**TL (cm)**	**TP**
Blenniidae	*Parablennius sanguinolentus*	PS	Herbivore	6	22	3	8.5–12.9	3.5	3	7.9–8.9	5.3	0	–	––
Gobiidae	*Gobius incognitus*	GI	Invertivore	6	10	5	7.3–8.1	3.4	5	7.1–11.3	3.4	5	6.8–9.7	3.3
Labridae	*Coris julis*	CJ	Invertivore	5	28	4	10.2–18.1	3.4	4	11.0–15.8	3.5	4	10.2–16.6	3.6
	Labrus viridis	LV	Invertivore	5	50	3	10.3–12.2	3.8	0	–	–	3	9.7–11.4	3.7
	Symphodus mediterraneus	SM	Invertivore	5	18	4	8.2–10.3	3.4	0	–	–	4	9.4–11.0	3.7
	Symphodus ocellatus	SO	Invertivore	5	12	6	6.2–7.5	3.6	6	5.3–7.5	3.7	3.7	-	-
	Symphodus roissali	SR	Invertivore	5	17	3	8.3–10.5	3.8	3	6.8–8.7	3.3	3	8.0–9.7	3.7
	Symphodus tinca	ST	Invertivore	5	35	4	9.7–16.0	3.3	4	8.1–13.5	3.7	4	9.8–18.7	3.4
	Thalassoma pavo	TP	Invertivore	5	25	5	10.0–11.4	3.4	5	10.5–14.6	4.0	5	11.5–14.5	3.7
Pomacentridae	*Chromis chromis*	CC	Planktivore	2	15	6	5.9–11.1	3.4	6	6.0–10.5	3.3	6	5.3–9.4	3.2
Scorpenidae	*Scorpaena porcus*	SCO	Small piscivore	6	30	3	9.2–14.0	3.2	3	12.4–15.0	3.6	3	10.2–16.2	3.3
Serranidae	*Serranus scriba*	SCR	Small piscivore	5	36	3	14.2–16.2	3.7	3	10.3–11.9	3.5	3	11.4–17.1	3.7
Sparidae	*Diplodus vulgaris*	DV	Invertivore	3	45	4	8.8–14.8	3.2	4	7.4–13.0	3.4	4	8.7–9.0	3.5
	Oblada melanura	OM	Planktivore	1	30	3	10.0–11.1	3.6	3	8.0–12.0	3.6	3	7.3–10.7	3.5
	Sarpa salpa	SS	Herbivore	3	50	4	16.7–18.0	3.1	4	21.5–24.5	3.0	4	15.8–27.5	3.0

* Harmelin (1987) grouped fish into spatial categories schematised the spatial organisation of Mediterranean ichthyofauna by defining six home-range categories varying along a mobility gradient from high-mobility pelagic fish to sedentary benthic fish: 1) high mobility species, living in large schoals in the water column; 2) schoaling species occupying the water column, but with low horizontal mobility; 3) mesophagous demersal species with important horizontal and moderate vertical displacements (mainly Sparids); 4) nekto-benthic species living close to the bottom and showing very wide horizontal displacements; 5) relatively sedentary mesophagous species; 6) small, site-attached very sedentary species.

$$TP_{consumer} = \left(\delta^{15}N_c - \delta^{15}N_b\right)/3.4 + x$$

where $\delta^{15}N_c$ and $\delta^{15}N_b$ are the nitrogen isotope values of the consumer and the baseline species respectively, 3.4 (‰) is the average ^{15}N-enrichment per trophic position and x is the trophic position of the baseline species, set to 2 (Post, 2002).

Because mercury accumulation in fish is strongly size-dependent, THg concentrations were normalised for body size to allow comparisons of trophic transfer independent of individual growth effects (Dang and Wang, 2012). Size-adjusted mercury concentrations (THg_{adj}) were obtained by regressing THg against total length for each species, following Garcia and Carignan (2005), using a general linear mixed model (GLMM with gaussian family and log link) and used as the response variable in all subsequent trophic transfer analyses. GLMMs are particularly appropriate when dealing with different species because observations are typically not independent across species. Individuals belonging to the same species tend to share biological, ecological, or evolutionary characteristics, which can introduce correlation in the data (Thorson and Minto, 2015). This approach improves the accuracy and generalizability of the results, as it properly partitions within-species and between-species variation.

To evaluate the effect of fish trophic position (TP) on THg_{adj} accumulation under contrasting pH conditions, and to test whether functional traits explain trophic transfer patterns better than species identity, a mixed-modelling framework based on GLMM (with gaussian family) was adopted. Specifically, the effect of TP on THg_{adj} accumulation and whether this effect varied between sites (Low pH *vs.* reference pH) was modelled. To account for biological variability at different levels of organisation (species *vs.* functional traits), two alternative random effects were used to test whether species identity or functional traits better explains THg_{adj} trophic transfer patterns. The first estimated model (hereafter referred as the *species-based model*) was:

$$\log\left(THg_{adj}\right) = \beta_0 + \beta_1 TP + \beta_2 LowpH + \beta_3 LowpH{\cdot}TP + random\,(Species)$$

where THg_{adj}concentration is the dependent variable (response variable), trophic position (TP) and reference sites are the independent variables, and species identity (Species) is used as a random factor to account for interspecific variability in THg accumulation.

In the second model (hereafter referred as the *trait-based model*), fish species were grouped according to unique combinations of mobility and trophic group (see Table 1), which were included as a random factor to account for functional trait-driven variability:

$$\log\left(THg_{adj}\right) = \beta_0 + \beta_1 TP + \beta_2 LowpH + \beta_3 LowpH{\cdot}TP + random\left(Trophic\_group/Mobility\right)$$

$$\log\left(THg_{adj}\right) = \beta_0 + \beta_1 TP + \beta_2 LowpH + \beta_3 LowpH{\cdot}TP + random\left(Trophic\_group\,/\,Mobility\right)$$

In both the estimated models, only fish species common to all sites were included to ensure comparability across conditions, and the two reference sites were combined to increase the sample size of the control group. This improves the statistical power of tests, reducing the chance of Type II errors (failing to detect a real effect; Cohen, 1988).

Finally, trophic magnification factor (TMF), representing the THg biomagnification power across trophic positions was calculated for each site from the slope of the regression equation of $\delta^{15}N$ *vs.* log-transformed THg concentration according to the formula: $TMF = 10^b$ (Nfon et al., 2009). TMF > 1 suggests biomagnification, while TMF < 1 suggests biodilution (Nfon et al., 2009).

R software (version 4.1.2) was used for all graphs ('ggplot2' package) and for calculating generalised linear mixed-effects models ('MASS' package). Data exploration was performed by R software using the ten-step protocol (Zuur and Ieno, 2016).

3. Results

Sediments and macroalgae showed comparable total mercury (THg) concentrations and a similar spatial trend with higher values at the Low

pH than at both reference sites (Fig. 2), while the seagrass *Cymodocea nodosa* differed between the three sites (Low pH > Ctrl 1 > Ctrl 2) (Fig. 2). Zooplankton showed a different spatial pattern than basal sources, with higher values at Ctrl 2 than at Low pH and Ctrl 1 sites (Fig. 2).

Fifteen fish species belonging to seven families (Blenniidae, Gobiidae, Labridae, Pomacentridae, Scorpenidae, Serranidae, Sparidae), four trophic groups (herbivores, planktivores, invertivores and small piscivores) and five mobility (1: highly mobile species living in large schoals in the water column; 2: schoaling species occupying the water column, but with little horizontal mobility; 3: mesophagous demersal species with large horizontal and moderate vertical displacements (mainly Sparids); 5: relatively sedentary mesophagous species; 6: small, site-attached very sedentary species) were collected at the low pH site and two reference sites (Table 1). Most species were invertivorous and relatively sedentary mesophagous species (group 5). Almost all species were common to the three sites, except for *Labrus viridis*, *Parablennius sanguinolentus, Symphodus mediterraneus* and *Symphodus ocellatus* which were found only at the Low pH site and at one of the two reference sites (Table 1).

Overall, fish species showed distinct species-specific accumulation patterns, with six (*Coris julis*, *Sarpa salpa, Serranus scriba*, *S. mediterraneus, S. ocellatus* and *Symphodus roissali*) of the fifteen analysed species showing higher THg at Low pH than at reference sites (Fig. 3A; Table 2). *Coris julis* showed comparable THg concentrations between Low pH and Ctrl 1, and both higher than Ctrl 2 (Fig. 3A; Table 2). Regarding functional traits, fish classified by trophic groups, herbivores, invertivores and small piscivores reflected the trend found in basal organic matter sources, with significantly higher THg levels at Low pH than at both reference sites (Fig. 3B; Table 2). In contrast, planktivores showed comparable THg concentrations at all sites and high variability at both reference sites (Fig. 3B; Table 2). For fish grouped by mobility, group 3 and group 5 showed higher THg/TP concentrations at Low pH than at both reference sites, while group 6 showed higher THg/TP at Low pH than Ctrl 1 (Fig. 3C; Table 2).

Comparison of THg concentrations with the European Union Maximum Residue Limits (MRLs) for species of commercial interest (four of the fifteen species analysed in this study), showed that *Scorpaena porcus* (THg = 0.06 ± 0.02, 0.05 ± 0.003 and 0.04 ± 0.02 mg kg^{-1} ww in Low pH, Ctrl 1 and Ctrl 2 respectively), *Diplodus vulgaris* (THg = 0.01 ± 0.005, 0.01 ± 0.02 mg kg^{-1} ww in Low pH, and both Ctrl 1 and Ctrl 2 respectively), *Oblada melanura* (THg = 0.02 ± 0.01, 0.02 ± 0.001 and 0.02 ± 0.01 mg kg^{-1} ww in Low pH, Ctrl 1 and Ctrl 2 respectively), and *S. salpa* (THg = 0.01 ± 0.003, 0.01 ± 0.004 and 0.004 ± 0.002 mg kg^{-1} ww in Low pH, Ctrl 1 and Ctrl 2 respectively) were always below the MRL (0.5 mg kg^{-1} ww, Regulation EC, N. 2023/915; Magalhães et al., 2007).

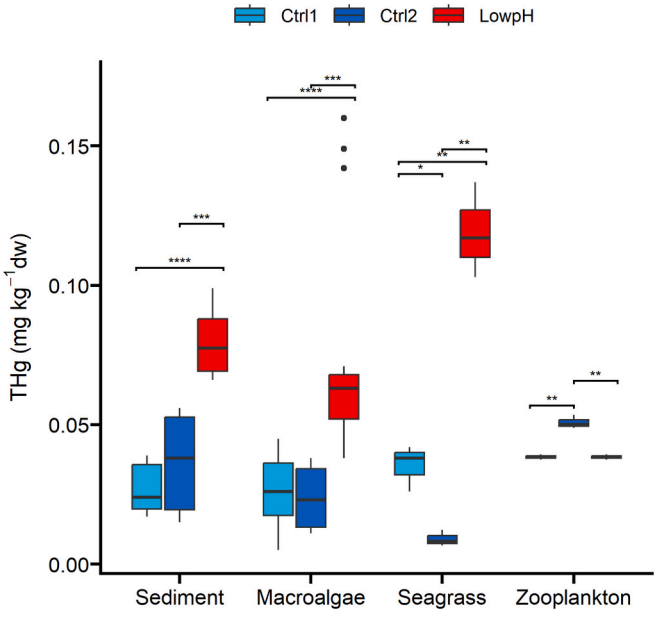

Fig. 2. - Concentration of THg (mg kg^{-1} dw) in basal organic matter sources (sediments, macroalgae, seagrasses) and low order consumers (zooplankton) at the three sampling sites (Ctrl 1, Ctrl 2 and Low pH). Significant codes: '****' 0.0001, '***' 0.001, '**' 0.01, '*' 0.05.

Generalised linear mixed models (GLMM) showed that the effect of the trophic position on the size-adjusted Hg (THg_{adj}) concentration varied significantly between sites at different pH in both models (Fig. 4). In particular, in the species-based model, the effect was positive and was higher in the Low pH than in the two combined reference sites (β_5 = 0.570 SE = 0.189, $p = 0.003$, Table 3, Fig. 4A). Species, used as a random factor in the model, accounted for only 50% of the variance. In the trait-based model, the effect was positive and was higher in the Low pH than in the two combined reference sites (β_5 = 0.604 SE = 0.187, $p = 0.002$, Table 3, Fig. 4B). Unique combination of mobility and trophic groups, used as a random factor in the model, accounted for about 90% of the variance. Finally, the trophic magnification factor (TMF) was higher in the Low pH site (1.75) than in either reference site (1.36 and 1.35 in Ctrl 1 and Ctrl 2, respectively).

4. Discussion

The forecasted decrease in ocean pH over the coming decades (*IPCC*, 2023) is a global climate-related threat that is expected to affect biodiversity, with consequences for ecosystem functioning and services (Zeng et al., 2015; Falkenberg et al., 2020). Although CO_2 vents are considered natural laboratories for testing the effects of ocean acidification (OA) on marine organisms due to their long-term exposure to high pCO_2/low pH conditions, these ecosystems can also provide an opportunity to study the combined effect of OA and trace element contamination as the typical reducing conditions favour the bioavailability and bioaccumulation of trace elements which are present in volcanic fluids (Kádár et al., 2005, 2007; Martins et al., 2006).

First, we assessed whether fish at the vent site were exposed to higher THg levels than at reference sites. Our results confirm the spatial pattern of THg contamination found by Vizzini et al. (2013) in the same study area, demonstrating that higher THg concentrations occurred in sediments and macrophytes (*i.e.*, macroalgae and seagrasses) at the low pH site near the shallow CO_2 vent in Levante Bay than at reference sites. In particular, Vizzini et al. (2013) found high trace element contamination (As, Ba, Mo, Ni, Pb, Hg, and Zn) and poor environmental quality at a distance between 150 and 350 m from the CO_2 vent (*i.e.*, within which the low pH site of this study falls), followed by an overall decrease at greater distances. The spatially localised contamination close to the vent resulted from the direct volcanic input of Hg into the environment and its high bioavailability due to the acidic and reducing sediment conditions (Roberts and Pichler, 2022), confirms the importance of explicitly considering the relevant spatial scale when investigating contaminant dynamics in acidified areas, in line with the recommendations of Zurlini et al. (2025). In contrast, the lower THg concentrations found in zooplankton near the vent than at one reference site may suggest a more efficient Hg detoxification mechanism under OA conditions, as observed by Wang et al. (2021) who found a reduction in Hg accumulation and associated toxicity in copepods exposed to long-term OA conditions. However, THg levels found in zooplankton in the Aeolian Archipelago are in line with those found in other Mediterranean sites (for a review see Boldrocchi et al., 2023).

We then investigated whether fish functional traits (trophic group and mobility) could better explain patterns of contaminant bioaccumulation than species identity under contrasting pH conditions, revealing that THg concentration were more consistently explained by trophic group and mobility than by species identity, in line with

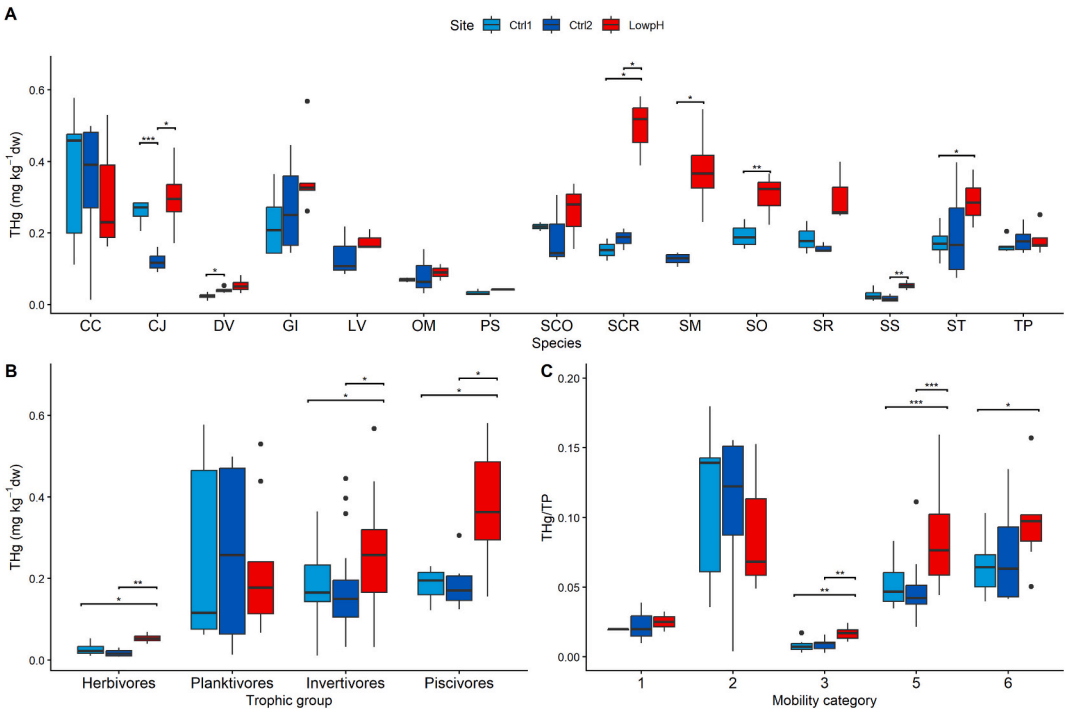

Fig. 3. – Concentration of total mercury THg (mg kg^{-1} dw) in fish at species level (A), grouped in trophic groups (B) and by mobility categories, with Hg normalised to trophic position THg/TP (C), at the three sampling sites (Ctrl 1, Ctrl 2 and Low pH). Fish are labelled as follows: CC, *Chromis chromis*; CJ, *Coris julis*; DV, *Diplodus vulgaris; GI, Gobius incognitus*; LV, *Labrus viridis*; OM, *Oblada melanura*; PS, *Parablennius sanguinolentus*; SCO, *Scorpaena porcus;* SCR, *Serranus scriba;* SM, *Symphodus mediterraneus*; SO, *Symphodus ocellatus*; SR, *Symphodus roissali*; SS, *Sarpa salpa*; ST, *Symphodus tinca* TP, *Thalassoma pavo*. For further information about species trophic groups and mobility categories see Table 1. The central line is the median, the whiskers indicate the variability outside the first and third quartile, while the dots are the outliers. Asterisks indicate the significance level of the differences: '****' 0.0001, '***' 0.001, '**' 0.01, '*' 0.05.

previous studies (Short et al., 2008; Signa et al., 2017).

At the species level, only six (*i.e.*, *Coris julis, Sarpa salpa*, *Serranus scriba*, *Symphodus mediterraneus*, *Symphodus ocellatus* and *Symphodus tinca*) out of the fifteen species analysed mirrored the spatial pattern observed in benthic sources (*i.e.*, higher THg levels at the vent site than at reference pH sites). The variable species-level responses likely reflect differences in exposure mostly linked to diet, mobility (Short et al., 2008; Signa et al., 2017), and time (Copat et al., 2012), further supporting the use of functional trait-based approaches over species identity alone for identifying effective indicators of trace element contamination in acidified areas.

Notable is the case of *C. julis,* which showed higher THg concentrations at the Low pH and Ctrl 1 sites than at Ctrl 2, most probably due to its high mobility and habitat use plasticity, including the use of the nearby reference site (Ctrl 1) as a 'recovery area' (*sensu* Mirasole et al., 2020) to escape stressful environmental conditions occurring at the Low pH site. The case of *S. salpa* is also particularly interesting as it represents the most important herbivorous fish species in the Mediterranean Sea and one of the most abundant fish species associated with seagrass systems in Mediterranean CO_2 vents (Mirasole et al., 2020, 2021b). Although herbivores are not considered effective accumulators of trace elements due to their low trophic position (Nfon et al., 2009), the higher THg accumulation observed near the Vulcano vent than at reference sites may be related to the functional role of *S. salpa* as a much active grazer with high herbivory rates (Mirasole et al., 2021b) promoted by the increased palatability of seagrasses under acidified conditions (Arnold et al., 2012). However, by comparing the THg concentration found in *S. salpa* with the EU maximum residue limits MRLs (0.5 mg kg^{-1} ww, according to Regulation EC, N. 2023/915; Magalhães et al., 2007), no threat to human consumption was detected. A similar result was found for other species of economic interest such as *D. vulgaris, O. melanura* and *S. porcus*.

Fish mobility is a key functional trait influencing the uptake and accumulation of trace elements, as it reflects habitat use and, therefore, the reliance on site-specific trophic resources (Mirasole, 2017; Signa et al., 2017). Consistently, only high mobility species, represented by zooplanktivores, showed spatial homogeneity in THg levels. On the contrary, demersal species belonging to mobility categories 3 (relatively mobile species, mainly Sparids), 5 (relatively sedentary species, mainly Labrids) and 6 (very sedentary species) (Harmelin, 1987), and represented by herbivores, invertivores and small piscivores, showed overall higher THg concentration at the Low pH site. This pattern mirrors the local contamination of benthic sources, emphasizing how mobility and small-scale habitat use, rather than species identity alone, influence contaminant transfer (Signa et al., 2017). This is also consistent with previous evidence that the large variation in Hg concentrations in aquatic and marine biota primarily reflects differences in bioconcentration at the base of the food web (Wu et al., 2019). The anemone goby *G. incognitus*, a small highly territorial and abundant fish in the vent area of Vulcano Island (Nagelkerken et al., 2015), represented a notable exception. Although it's extremely sedentary behaviour and benthic feeding mode, no significant spatial differences in THg concentrations were found, suggesting the presence of efficient detoxification and/or excretion mechanisms under chronic contaminant exposure (Suggett et al., 2012). Although high pCO_2/low pH conditions have been associated with skeletal pre-ageing in *G. incognitus* from the study area (Mirasole et al., 2021a), acclimation mechanisms may partly explain its population success under OA conditions (Suresh et al., 2023).

Both mixed-effects models (species-based and trait-based) consistently showed a stronger relationship between fish trophic position and THg concentration at the Low pH site than at the reference sites, in agreement with the higher trophic magnification factor (TMF) estimated for the vent site, indicating enhanced trophic transfer and biomagnification through the fish food web. Importantly, the model accounting for functional groups (mobility × trophic group) explained a much larger proportion of variance (~90%) than the species-based

Table 2
Summary of THg (mg kg^{-1} dw) and $\delta^{15}N$ (‰) values as mean (± SD) measured in sediment, macroalgae, seagrass, zooplankton and fish sampled in the three sites (Low pH, Ctrl 1 and Ctrl 2).

Basal organic matter source / *fish species*	Low pH		Ctrl 1		Ctrl 2	
	THg	**$\delta^{15}N$**	**THg**	**$\delta^{15}N$**	**THg**	**$\delta^{15}N$**
Sediment	0.08 (0.01)	–	0.03 (0.01)	–	0.04 (0.001)	–
Macroalgae	0.07 (0.04)	–	0.03 (0.01)	–	0.02 (0.01)	–
Seagrass	0.12 (0.02)	–	0.04 (0.01)	–	0.01 (0.001)	–
Zooplankton	0.04 (0.001)	1.9 (0.1)	0.05 (0.001)	1.9 (0.1)	0.04 (0.001)	2.4 (0.4)
Chromis chromis	0.29 (0.15)	6.5 (0.4)	0.37 (0.20)	6.1 (0.2)	0.34 (0.19)	6.6 (0.6)
Coris julis	0.30 (0.11)	6.8 (0.2)	0.26 (0.04)	7.2 (0.3)	0.12 (0.03)	7.6 (0.2)
Diplodus vulgaris	0.05 (0.02)	6.3 (1.0)	0.02 (0.01)	7.0 (1.0)	0.04 (0.01)	7.4 (0.5)
Gobius incognitus	0.36 (0.12)	6.9 (0.6)	0.23 (0.09)	6.8 (0.8)	0.27 (0.13)	6.6 (0.4)
Labrus viridis	0.18 (0.03)	8.0 (0.1)	–	–	0.14 (0.07)	8.2 (0.1)
Oblada melanura	0.09 (0.02)	7.6 (0.4)	0.07 (0.01)	7.4 (0.9)	0.08 (0.06)	7.1 (1.6)
Parablennius sanguinolentus	0.04 (0.001)	8.0 (2.5)	0.03 (0.01)	13.1 (3.2)	–	–
Sarpa salpa	0.05 (0.01)	5.9 (0.3)	0.03 (0.02)	5.6 (0.4)	0.02 (0.01)	5.6 (0.2)
Scorpaena porcus	0.26 (0.09)	6.3 (0.4)	0.22 (0.01)	7.5 (1.0)	0.19 (0.10)	6.5 (0.8)
Serranus scriba	0.50 (0.10)	8.0 (0.6)	0.15 (0.03)	7.3 (0.1)	0.18 (0.03)	7.9 (0.4)
Symphodus mediterraneus	0.38 (0.13)	6.7 (0.3)		–	0.13 (0.02)	6.6 (0.1)
Symphodus ocellatus	0.31 (0.05)	7.4 (0.4)	0.19 (0.03)	7.6 (0.1)	–	–
Symphodus tinca	0.29 (0.07)	6.5 (0.5)	0.17 (0.05)	7.9 (1.2)	0.20 (0.15)	7.0 (0.5)
Thalassoma pavo	0.18 (0.04)	6.9 (0.2)	0.17 (0.02)	9.1 (0.7)	0.18 (0.04)	7.9 (0.2)

model (~50%), confirming that Hg bioaccumulation patterns are better captured by functional organisation of food webs than by species identity alone. At the vent site, both models showed a strong positive relationship between trophic position and THg, consistent with enhanced Hg bioavailability and dietary transfer promoted by acidified conditions. Such physicochemical characteristics are known to increase metal solubility and uptake at the base of aquatic food webs, thereby amplifying biomagnification processes (Jardine et al., 2013; Wu et al., 2019). In contrast, in the reference conditions, both models revealed a weak or negative relationship between trophic position and THg, suggesting that biomagnification may be weak or absent. In such conditions, particularly when baseline Hg levels are low and more homogeneous across organic matter sources, Hg concentrations may not systematically increase across trophic position, as previously observed in fish assemblages characterised by low background contamination (Jardine et al., 2013; Amundsen et al., 2023). While Hg biomagnification is well documented in marine food webs (*e.g.*, Nfon et al., 2009; Signa et al., 2017, 2019), including studies focusing exclusively on fish assemblages (Amundsen et al., 2023; Nalley et al., 2023), our results highlights that

Table 3
- Summary of generalised linear mixed models (GLMMs) assessing changes in size-adjusted total mercury (THg_{adj}) along trophic positions under contrasting pH conditions (sites), accounting for a) taxonomic variability (*species-based model*) and b) functional variability (*trait-based model*).

a) Species-based model

Predictors	Estimate	Std. Error	df	t-value	*p*-value
(Intercept)	−1.961	0.432	118	−4.532	0.000
Trophic Position (TP)	0.039	0.111	118	0.351	0.726
Site = Low pH	−1.953	0.644	118	−3.031	**0.003**
TP*Low pH	0.570	0.189	118	3.023	**0.0031**

b) Trait-based model

Predictors	Estimate	Std. Error	df	t-value	p-value
(Intercept)	−1.702	0.455	121	−3.74	0.0003
Trophic Position (TP)	−0.059	0.108	121	−0.549	0.583
Site = Low pH	−2.074	0.638	121	−3.250	**0.002**
TP*Low pH	0.604	0.187	121	3.233	**0.002**

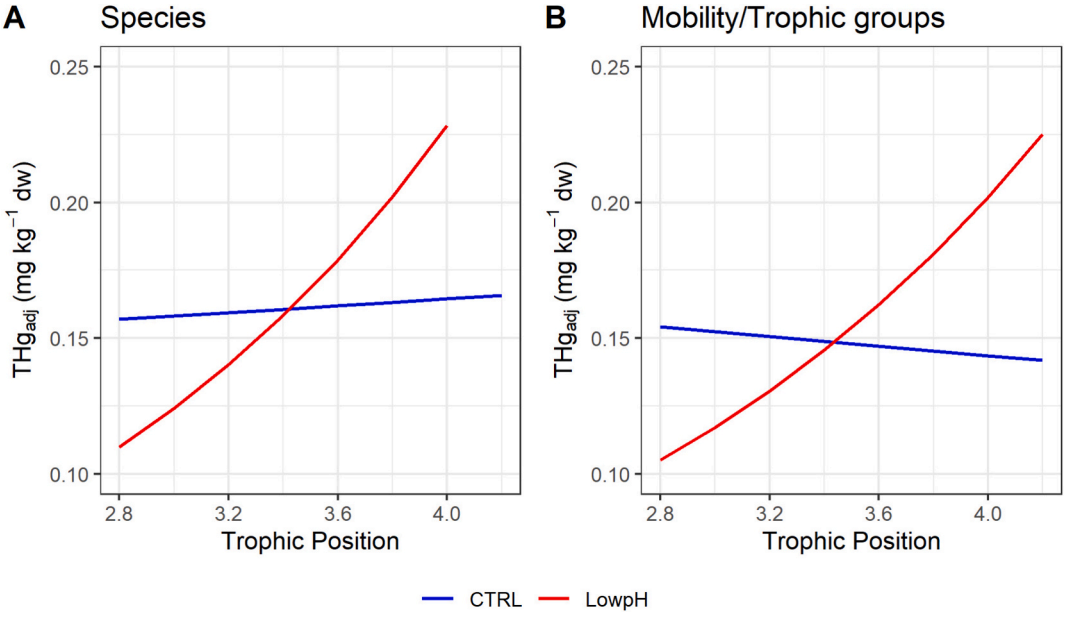

Fig. 4. - Interaction plot between the trophic position and size-adjusted total mercury (THg_{adj}) concentration (mg kg^{-1} dw) of the two models of fish species common to sampling sites (blue line: combined reference with ambient pH sites; red line: Low pH site). a) GLMM with species as a random factor; b) GLMM with unique combinations of functional traits (mobility and trophic groups) as a random factor. (For interpretation of the references to colour in this figure legend, the reader is referred to the web version of this article.)

biomagnification is not an intrinsic property of food webs, but an emergent process primarily driven by combined contaminant availability and functional trophic traits. In addition, interactions with other dissolved elements may also influence Hg dynamics and deserve further investigation.

5. Conclusion

Localised mercury (Hg) contamination was found in sediments and benthic basal sources near the primary CO_2 vent of Levante Bay (Vulcano Island, Italy). Although differences in total mercury (THg) among fish species were detected, THg patterns were more consistently explained by functional traits, namely trophic group and mobility, than by species identity alone. Low-mobility benthic fish exhibited higher THg concentrations at the vent site, whereas highly mobile shoaling species did not, indicating a clear spatial gradient of exposure, linked to functional pathways. Also, trophic position played a stronger role in THg transfer in the low pH site, suggesting enhanced bioaccumulation and biomagnification under elevated Hg availability. However, heterogeneous species responses highlight the key role of functional traits in mediating Hg transfer. Conversely, weak or absent biomagnification under reference conditions reflects low baseline Hg availability, indicating that Hg trophic transfer is an emergent property dependent on contaminant availability and functional organisation of the food-web rather than an intrinsic feature of food webs. Importantly, the higher explanatory power of the functional-trait model further supports functional trophic position as a mechanistic framework for predicting contaminant dynamics.

Moreover, although only total Hg was analysed, likely resulting in conservative estimates of biomagnification, and the experimental design did not allow to separate the effects of ocean acidification and Hg contamination, the results suggest that in future acidified and polluted seas, increased Hg bioavailability, bioaccumulation and biomagnification can be expected. Finally, given the usefulness of CO_2 vents as natural analogues of future ocean conditions, further studies using a functional-trait-based and multi-scale perspective and explicitly accounting for spatial and temporal variation in exposure, can improve biomonitoring and forecasting of trace element dynamics in acidified marine ecosystems.

CRediT authorship contribution statement

Alice Mirasole: Writing – review & editing, Writing – original draft, Visualization, Investigation, Formal analysis, Data curation, Conceptualization. **Geraldina Signa:** Writing – review & editing, Visualization, Validation, Methodology, Investigation, Formal analysis, Data curation. **Giovanna Cilluffo:** Writing – review & editing, Visualization, Validation, Methodology, Formal analysis, Data curation. **Cecilia Tramati:** Writing – review & editing, Formal analysis. **Agostino Tomasello:** Writing – review & editing, Validation, Investigation. **Antonio Mazzola:** Writing – review & editing, Resources, Funding acquisition. **Salvatrice Vizzini:** Writing – review & editing, Supervision, Project administration, Investigation, Funding acquisition, Data curation, Conceptualization.

Ethical approval

All applicable international, national, and/or institutional guidelines for the care and use of animals were followed.

Declaration of competing interest

The authors declare that they have no known competing financial interests or personal relationships that could have appeared to influence the work reported in this paper.

Acknowledgements

The authors wish to thank Andrea Savona, Antonino M. Vaccaro and Giulia Visconti for help during field activities and Alessandro Aglialoro for laboratory activities. This study was supported by Strategia Marina, Accordo di Ricerca tra ISPRA e CoNISMa del 18.11.2024, the University of Palermo (FFR) and the European Union Next-Generation EU (National Recovery and Resilience Plan – NRRP, Mission 4, Component 2, Investment 1.3 – D.D. 1243 2/8/2022, PE0000005) in the framework of the RETURN Extended Partnership.

Data availability

Data will be made available on request.

References

Aiuppa, A., Hall-Spencer, J.M., Milazzo, M., Turco, G., Caliro, S., Di Napoli, R., 2021. Volcanic CO_2 seep geochemistry and use in understanding ocean acidification. Biogeochemistry 152 (1), 93–115. https://doi.org/10.1007/s10533-020-00737-9.

Amundsen, P.A., Henriksson, M., Poste, A., Prati, S., Power, M., 2023. Ecological drivers of mercury bioaccumulation in fish of a subarctic watercourse. Environ. Toxicol. Chem. 42 (4), 873–887. https://doi.org/10.1002/etc.5580.

Andolina, C., Cilluffo, G., Zammuto, V., Signa, G., Papale, M., Giudice, A.L., Di Leonardo, R., Costa, V., Ciriminna, L., Tomasello, A., Gugliandolo, C., Vizzini, S., 2025. Extreme abiotics drive sediment biocomplexity along pH gradients in a shallow submarine volcanic vent. Mar. Poll. Bull. 211, 117470. https://doi.org/10.1016/j.marpolbul.2024.117470.

Apostolaki, E.T., Vizzini, S., Hendriks, I., Olsen, Y.S., 2014. Seagrass ecosystem response to long-term high CO_2 in a Mediterranean volcanic vent. Mar. Environ. Res. 99, 9–15. https://doi.org/10.1016/j.marenvres.2014.05.008.

Ardelan, M.V., Sundeng, K., Slinde, G.A., Gjøsund, N.S., Nordtug, T., Olsen, A.J., Torp, T. A., 2012. Impacts of possible CO_2 seepage from sub-seabed storage on trace elements mobility and bacterial distribution at sediment-water interface. Energy Procedia 23, 449–461. https://doi.org/10.1016/j.egypro.2012.06.047.

Arnold, T., Mealey, C., Leahey, H., Miller, A.W., Hall-Spencer, J.M., Milazzo, M., Maers, K., 2012. Ocean acidification and the loss of phenolic substances in marine plants. PLoSOne 7, e35107. https://doi.org/10.1371/journal.pone.0035107.

Basallote, M.D., De Orte, M.R., Del Valls, T.A., Riba, I., 2014. Studying the effect of CO_2-induced acidification on sediment toxicity using acute amphipod toxicity test. Environ. Sci. Technol. 48 (15), 8864–8872. https://doi.org/10.1021/es5015373.

Boatta, F., D'Alessandro, W., Gagliano, A.L., Liotta, M., Milazzo, M., Rodolfo-Metalpa, R., Hall-Spencer, J.M., Parello, F., 2013. Geochemical survey of Levante Bay, Vulcano Island (Italy), a natural laboratory for the study of ocean acidification. Mar. Pollut. Bull. 73, 485–494. https://doi.org/10.1016/j.marpolbul.2013.01.029.

Boldrocchi, G., Villa, B., Monticelli, D., Spanu, D., Magni, G., Pachner, J., Bettinetti, R., 2023. Zooplankton as an indicator of the status of contamination of the Mediterranean Sea and temporal trends. Mar. Poll. Bull. 197, 115732. https://doi.org/10.1016/j.marpolbul.2023.115732.

Brambilla, G., Abete, M.C., Binato, G., Chiaravalle, E., Cossu, M., Dellatte, E., Miniero, R., Orletti, R., Piras, P., Roncarati, A., Ubaldi, A., Chessa, G., 2013. Mercury occurrence in Italian seafood from the Mediterranean Sea and possible intake scenarios of the Italian coastal population. Regul. Toxicol. Pharmacol. 65 (2), 269–277. https://doi.org/10.1016/j.yrtph.2012.12.009.

Byrne, R.H., 2002. Inorganic speciation of dissolved elements in seawater: the influence of pH on concentration ratios. Geochem. T. 2 (2), 11. https://doi.org/10.1039/B109732F.

Campbell, L.M., Norstrom, R.J., Hobson, K.A., Muir, D.C., Backus, S., Fisk, A.T., 2005. Mercury and other trace elements in a pelagic Arctic marine food web (Northwater polynya, Baffin Bay). STOTEN 351, 247–263. https://doi.org/10.1016/j.scitotenv.2005.02.043.

Castro-González, M.I., Méndez-Armenta, M., 2008. Heavy metals: implications associated to fish consumption. Environ. Toxicol. Phar. 26 (3), 263–271. https://doi.org/10.1016/j.etap.2008.06.001.

Cohen, J., 1988. Statistical Power Analysis for the Behavioral Sciences, 2nd ed. Routledge. https://doi.org/10.4324/9780203771587.

Copat, C., Bella, F., Castaing, M., Fallico, R., Sciacca, S., Ferrante, M., 2012. Heavy metals concentrations in fish from Sicily (Mediterranean Sea) and evaluation of possible health risks to consumers. Bull. Environ. Contam. Toxicol. 88, 78–83. https://doi.org/10.1007/s00128-011-0433-6.

Cossa, D., Knoery, J., Bănaru, D., Harmelin-Vivien, M., Sonke, J.E., Hedgecock, I.M., Heimbürger-Boavida, L.E., 2022. Mediterranean mercury assessment 2022: an updated budget, health consequences, and research perspectives. Environ. Sci. Tech. 56 (7), 3840–3862. https://doi.org/10.1021/acs.est.1c03044.

Dang, F., Wang, W.X., 2012. Why mercury concentration increases with fish size? Biokinetic explanation. Env. Poll. 163, 192–198. https://doi.org/10.1016/j.envpol.2011.12.026.

Doney, S.C., Fabry, V.J., Feely, R.A., Kleypas, J.A., 2009. Ocean acidification: the other CO_2 problem. Ann. Rev. Mar. Sci. 1, 169–192. https://doi.org/10.1146/annurev.marine.010908.163834.

Falcone, E.E., Federico, C., Boudoire, G., 2022. Geochemistry of trace metals and rare earth elements in shallow marine water affected by hydrothermal fluids at Vulcano (Aeolian Islands, Italy). Chem. Geol. 593, 120756. https://doi.org/10.1016/j.chemgeo.2022.120756.

Falkenberg, L.J., Bellerby, R.G., Connell, S.D., Fleming, L.E., Maycock, B., Russell, B.D., Dupont, S., 2020. Ocean acidification and human health. Int. J. Environ. Res. Public Health 17 (12), 4563.

Froese, R., Pauly, D.. FishBase World Wide Web Electronic Publication. www.fishbase.org.

Garcia, E., Carignan, R., 2005. Mercury concentrations in fish from forest harvesting and fire-impacted Canadian boreal lakes compared using stable isotopes of nitrogen. Environ. Toxicol. Chem. 24 (3), 685–693. https://doi.org/10.1897/04-065r.1.

Gaylord, B., Kroeker, K.J., Sunday, J.M., Anderson, K.M., Barry, J.P., Brown, N.E., Connell, S.D., Dupont, S., Fabricius, K.E., Hall-Spencer, J.M., Klinger, T., Milazzo, M., Munday, P.L., Russell, B.D., Sanford, E., Schreiber, S.J., Thiyagarajan, V., Vaughan, M.L.H., Widdicombe, S., Harley, C.D., 2015. Ocean acidification through the lens of ecological theory. Ecology 96 (1), 3–15. https://doi.org/10.1890/14-0802.1.

Guidetti, P., Sala, E., 2007. Community-wide effects of marine reserves in the Mediterranean Sea. Mar. Ecol. Prog. Ser. 335, 43–56. https://doi.org/10.3354/meps335043.

Harmelin, J.G., 1987. Structure and variability of the ichthyofauna in a Mediterranean protected rocky area (National Park of port-Cros, France). Mar. Ecol. 8 (3), 263–284. https://doi.org/10.1111/j.1439-0485.1987.tb00188.x.

Climate change 2023: synthesis report. In: Lee, H., Romero, J., IPCC (Eds.), 2023. A report of the intergovernmental panel on climate change. Contribution of working groups I, II and III to the sixth assessment report of the intergovernmental panel on climate change [Core writing team]. IPCC, Geneva, Switzerland. https://doi.org/10.59327/IPCC/AR6-9789291691647.

Ivanina, A.V., Sokolova, I.M., 2015. Interactive effects of metal pollution and ocean acidification on physiology of marine organisms. Curr. Zool. 61 (4), 653–668. https://doi.org/10.1093/czoolo/61.4.653.

Jardine, T.D., Kidd, K.A., O'Driscoll, N., 2013. Food web analysis reveals effects of pH on mercury bioaccumulation at multiple trophic levels in streams. Aquatic. Toxicol. 132, 46–52. https://doi.org/10.1016/j.aquatox.2013.01.013.

Kádár, E., Costa, V., Martins, I., Santos, R.S., Powell, J.J., 2005. Enrichment in trace metals (Al, Mn, Co, Cu, Mo, Cd, Fe, Zn, Pb and Hg) of macro-invertebrate habitats at hydrothermal vents along the Mid-Atlantic Ridge. Hydrobiologia 548 (1), 191–205. https://doi.org/10.1007/s10750-005-4758-1.

Kádár, E., Costa, V., Segonzac, M., 2007. Trophic influences of metal accumulation in natural pollution laboratories at deep-sea hydrothermal vents of the mid-Atlantic ridge. STOTEN 373 (2), 464–472. https://doi.org/10.1016/j.scitotenv.2006.12.022.

Kroeker, K.J., Kordas, R.L., Crim, R., Hendriks, I.E., Ramajo, L., Singh, G.S., Duarte, C.M., Gattuso, J.P., 2013. Impacts of ocean acidification on marine organisms: quantifying sensitivities and interaction with warming. Glob. Change Biol. 19, 1884–1896. https://doi.org/10.1111/gcb.12179.

Lacoue-Labarthe, T., Martin, S., Oberhansli, F., Teyssie, J.L., Markich, S., Ross, J., Bustamante, P., 2009. Effects of increased pCO2 and temperature on trace element (Ag, Cd and Zn) bioaccumulation in the eggs of the common cuttlefish, *Sepia officinalis*. Biogeosciences 6 (11), 2561–2573. https://doi.org/10.5194/bg-6-2561-2009.

Lacoue-Labarthe, T., Reveillac, E., Oberhansli, F., Teyssie, J.L., Jeffree, R., Gattuso, J.P., 2011. Effects of ocean acidification on trace element accumulation in the early-life stages of squid *Loligo vulgaris*. Aquat. Toxicol. 105 (1), 166–176. https://doi.org/10.1016/j.aquatox.2011.05.021.

Lall, S.P., 2002. The minerals. In: Halver, J.E., Hardy, R.W. (Eds.), Fish Nutrition, 3rd edition. Academic Press Inc, San Diego, pp. 259–308.

Lewis, C., Ellis, R.P., Vernon, E., Elliot, K., Newbatt, S., Wilson, R.W., 2016. Ocean acidification increases copper toxicity differentially in two key marine invertebrates with distinct acid-base responses. Sci. Rep. 6 (1), 1–10. https://doi.org/10.1038/srep21554.

Magalhães, M.C., Costa, V., Menezes, G.M., Pinho, M.R., Santos, R.S., Monteiro, L.R., 2007. Intra-and inter-specific variability in total and methylmercury bioaccumulation by eight marine fish species from the Azores. Mar. Poll. Bull. 54 (10), 1654–1662. https://doi.org/10.1016/j.marpolbul.2007.07.006.

Martins, I., Costa, V., Porteiro, F.M., Colaço, A., Santos, R.S., 2006. Mercury concentrations in fish species caught at mid-Atlantic ridge hydrothermal vent fields. Mar. Ecol. Prog. Ser. 320, 253–258. https://doi.org/10.3354/meps320253.

Milazzo, M., Cattano, C., Alonzo, S.H., Foggo, A., Gristina, M., Rodolfo-Metalpa, R., Hall-Spencer, J.M., 2016. Ocean acidification affects fish spawning but not paternity at CO_2 seeps. Proc. R. Soc. B: Biol. 283 (1835), 20161021. https://doi.org/10.1098/rspb.2016.1021.

Mirasole, A., 2017. Structural and Functional Organization of Fish Assemblages in a Mediterranean Shallow CO_2 Vent. . In: PhD Thesis,. University of Palermo, p. 113.

Mirasole, A., Gillanders, B.G., Reis-Santos, P., Grassa, F., Capasso, G., Scopelliti, G., Mazzola, A., Vizzini, S., 2017. The influence of high pCO_2 on otolith shape, chemical and carbon isotope composition of six coastal fish species in a Mediterranean shallow CO_2 vent. Mar. Biol. 164 (9), 191. https://doi.org/10.1007/s00227-017-3221-y.

Mirasole, A., Signa, G., Gianguzza, P., Bonaviri, C., Mazzola, A., Vizzini, S., 2020. Fish assemblages cope with ocean acidification in a shallow volcanic CO_2 vent benefiting from an adjacent recovery area. Mar. Env. Res. 157, 104851. https://doi.org/10.1016/j.marenvres.2019.104851.

Mirasole, A., Scopelliti, G., Tramati, C., Signa, G., Mazzola, A., Vizzini, S., 2021a. Evidences on alterations in skeleton composition and mineralization in a site-attached fish under naturally acidified conditions in a shallow CO_2 vent. Sci. Total Environ. 761, 143309. https://doi.org/10.1016/j.scitotenv.2020.143309.

Mirasole, A., Badalamenti, F., Di Franco, A., Gambi, M.C., Teixidó, N., 2021b. Boosted fish abundance associated with *Posidonia oceanica* meadows in temperate shallow CO_2 vents. STOTEN 771, 145438. https://doi.org/10.1016/j.scitotenv.2021.145438.

Mishra, A.K., Santos, R., Hall-Spencer, J.M., 2020. Elevated trace elements in sediments and seagrasses at CO_2 seeps. Mar. Env. Res. 153, 104810. https://doi.org/10.1016/j.marenvres.2019.104810.

Nagelkerken, I., Russell, B.D., Gillanders, B.M., Connell, S.D., 2015. Ocean acidification alters fish populations indirectly through habitat modification. Nat. Clim. Chang. 6, 89–93. https://doi.org/10.1038/NCLIMATE2757.

Nalley, E.M., Pirkle, C.M., Schmidbauer, M.C., Lewis, C.J., Dacks, R.S., Thompson, M.D., Donahue, M.J., 2023. Trophic and spatial patterns of contaminants in fishes from the Republic of the Marshall Islands in the equatorial Pacific. Chemosphere 314, 137593. https://doi.org/10.1016/j.chemosphere.2022.137593.

Nfon, E., Cousins, I.T., Järvinen, O., Mukherjee, A.B., Verta, M., Broman, D., 2009. Trophodynamics of mercury and other trace elements in a pelagic food chain from the Baltic Sea. STOTEN 407 (24), 6267–6274. https://doi.org/10.1016/j.scitotenv.2009.08.032.

Nikinmaa, M., 2013. Climate change and ocean acidification—interactions with aquatic toxicology. Aquat. Toxicol. 126, 365–372. https://doi.org/10.1016/j.aquatox.2012.09.006.

Peña, V., Harvey, B.P., Agostini, S., Porzio, L., Milazzo, M., Horta, P., Hall-Spencer, J.M., 2021. Major loss of coralline algal diversity in response to ocean acidification. Glob. Change. Biol. 27 (19), 4785–4798. https://doi.org/10.1111/gcb.15757.

Pichler, T., 2024. Environmental inventory of mercury (Hg) for the marine shallow water hydrothermal system at Panarea, Italy. Sci. Total Environ. 911, 168575. https://doi.org/10.1016/j.scitotenv.2023.168575.

Post, D.M., 2002. Using stable isotopes to estimate trophic position: models, methods, and assumptions. Ecology 83, 703e718. https://doi.org/10.2307/3071875.

Power, M., Klein, G.M., Guiguer, K.R.R.A., Kwan, M.K.H., 2002. Mercury accumulation in the fish community of a sub-Arctic lake in relation to trophic position and carbon sources. J. Appl. Ecol. 39 (5), 819–830. https://doi.org/10.1046/j.1365-2664.2002.00758.x.

Roberts, H., Pichler, T., 2022. Hg in the hydrothermal fluids and gases in Baia di Levante, Vulcano, Italy. Mar. Chem. 244, 104147. https://doi.org/10.1016/j.marchem.2022.104147.

Roberts, D.A., Birchenough, S.N., Lewis, C., Sanders, M.B., Bolam, T., Sheahan, D., 2013. Ocean acidification increases the toxicity of contaminated sediments. Glob. Change. Biol. 19 (2), 340–351. https://doi.org/10.1111/gcb.12048.

Sampaio, E., Lopes, A.R., Francisco, S., Paula, J.R., Pimentel, M., Maulvault, A.L., Rosa, R., 2017. Ocean acidification dampens physiological stress response to warming and contamination in a commercially-important fish (*Argyrosomus regius*). STOTEN 618, 388–398. https://doi.org/10.1016/j.scitotenv.2017.11.059.

Shi, W., Zhao, X., Han, Y., Che, Z., Chai, X., Liu, G., 2016. Ocean acidification increases cadmium accumulation in marine bivalves: a potential threat to seafood safety. Sci. Rep. 6 (1), 1–8. https://doi.org/10.1038/srep20197.

Short, T.M., Deweese, L.R., Dubrovsky, N.M., 2008. Discrimination of trait-based characteristics by trace element bioaccumulation in riverine fishes. Can. J. Fish. Aquat. Sci. 65 (6), 1087–1100. https://doi.org/10.1139/F08-036.

Signa, G., Mazzola, A., Tramati, C.D., Vizzini, S., 2017. Diet and habitat use influence hg and cd transfer to fish and consequent biomagnification in a highly contaminated area: Augusta bay (Mediterranean Sea). Environ. Poll. 230, 394–404. https://doi.org/10.1016/j.envpol.2017.06.027.

Signa, G., Calizza, E., Costantini, M.L., Tramati, C., Sporta Caputi, S., Mazzola, A., Rossi, L., Vizzini, S., 2019. Horizontal and vertical food web structure drives trace element trophic transfer in Terra Nova Bay, Antarctica. Environ. Pollut. 246, 772–781. https://doi.org/10.1016/j.envpol.2018.12.071.

Suggett, D.J., Hall-Spencer, J.M., Rodolfo-Metalpa, R., Boatman, T.G., Pettay, D.T., Johnson, V.R., Warner, M.E., Lawson, T., 2012. Sea anemones may thrive in a high CO_2 world. Glob. Change. Biol. 18, 3015–3025. https://doi.org/10.1111/j.1365-2486.2012.02767.x.

Suresh, S., Mirasole, A., Ravasi, T., Vizzini, S., Schunter, C., 2023. Brain transcriptome of gobies inhabiting natural CO_2 seeps reveal acclimation strategies to long-term acidification. Evol. Appl. 16 (7), 1345–1358. https://doi.org/10.1111/eva.13574.

Thorson, J.T., Minto, C., 2015. Mixed effects: a unifying framework for statistical modelling in fisheries biology. ICES J.Mar. Sci. 72 (5), 1245–1256. https://doi.org/10.1093/icesjms/fsu213.

Tovar-Sanchez, A., Duarte, C.M., Hernández-León, S., Sañudo-Wilhelmy, S.A., 2009. Impact of submarine hydrothermal vents on the metal composition of krill and its excretion products. Mar. Chem. 113 (1), 129–136. https://doi.org/10.1016/j.marchem.2009.01.010.

Vizzini, S., Di Leonardo, R., Costa, V., Tramati, C.D., Luzzu, F., Mazzola, A., 2013. Trace element bias in the use of CO_2 vents as analogues for low pH environments:

implications for contamination levels in acidified oceans. Estuar. Coast. Shelf. 134, 19–30. https://doi.org/10.1016/j.ecss.2013.09.015.
Vizzini, S., Martínez-Crego, B., Andolina, C., Massa-Gallucci, A., Connel, S.D., Gambi, M. C., 2017. Ocean acidification as a driver of community simplification via the collapse of higher-order and rise of lower-order consumers. Sci. Rep. 7, 4018. https://doi.org/10.1038/s41598-017-03802-w.
Wang, M., Chen, J., Lee, Y.H., Lee, J.S., Wang, D., 2021. Projected near-future ocean acidification decreases mercury toxicity in marine copepods. Environ. Poll. 284, 117140. https://doi.org/10.1016/j.envpol.2021.117140.
Wu, P., Kainz, M.J., Bravo, A.G., Åkerblom, S., Sonesten, L., Bishop, K., 2019. The importance of bioconcentration into the pelagic food web base for methylmercury biomagnification: a meta-analysis. STOTEN 46, 357–367. https://doi.org/10.1016/j.scitotenv.2018.07.328.
Zeng, X., Chen, X., Zhuang, J., 2015. The positive relationship between ocean acidification and pollution. Mar. Poll. Bull. 91, 14–21. https://doi.org/10.1016/j.marpolbul.2014.12.001.
Zhang, L., Campbell, L.M., Johnson, T.B., 2012. Seasonal variation in mercury and food web biomagnification in Lake Ontario, Canada. Environ. Pollut. 161, 178–184. https://doi.org/10.1016/j.envpol.2011.10.023.
Zurlini, G., An, Y.J., Franklin, E., Hamalainen, H., Kaklauskas, A., Pert, P., Petrosillo, I., Sànchez-Pinillos, M., Selvan, T., Zuo, J., 2025. The crucial issue of spatial and temporal scale in ecological indication. Ecol. Indic. 174, 113466. https://doi.org/10.1016/j.ecolind.2025.113466.
Zuur, A.F., Ieno, E.N., 2016. A protocol for conducting and presenting results of regression-type analyses. Methods Ecol. Evol. 7 (6), 636–645. https://doi.org/10.1111/2041-210X.12577.